

# Determination of accuracy of particle size by acoustic scattering using a modified Born approximation

Ratan K Saha\*

LBUM-CRCHUM, University of Montreal, Canada

and

Subodh K Sharma

Satyendra Nath Bose National Centre for Basic Sciences, Block JD, Sector III, Salt Lake, Kolkata 700 098

Received 1 November 2007; accepted 16 May 2008

Accuracy of a recently proposed modified Born approximation (MBA) has been examined for size determination of an isolated scatterer. Two methods have been employed for this purpose. One is based on the analysis of the angular scattering pattern of plane waves and the other on analysis of the power spectrum of the backscattered pulse. In each case, domain of validity of the modified Born approximation for size determination has been assessed for two exactly soluble test models, namely, the scattering by a sphere and an infinitely long cylinder. For completeness, comparisons with conventional Born approximation (BA) results have also been made. The performances of the approximations have been examined for scatterers whose size parameters vary over a range 3 to 75. Mismatches of the density and compressibility are less than 15% in these calculations. Numerical results show that MBA indeed has a larger validity domain in comparison to BA for an intermediate size weak scatterer.

**Keywords:** Acoustic waves, Scattering, Born approximation, Particle sizing

## 1 Introduction

The techniques of back and angular acoustic wave scattering have been widely used to characterize a single scatterer as well as particles in a collection of scatterers<sup>1-5</sup>. For interpreting the scattering, whether from an isolated particle or a collection of particles, a pre-requisite is the knowledge of a theory that is capable of describing the scattering by a single scatterer. Exact analytic solutions for the problem of acoustic scattering by targets of regular geometry (*e. g.* sphere, long cylinder *etc.*) are available<sup>16,17</sup> and can be expressed in terms of the frequency of the incident wave, size of the scatterer and mismatch of density and compressibility of the scatterer and the surrounding medium. However, these solutions are in the form of infinite series and therefore relationship between the measured quantities and the physical parameters is not distinct. This makes it cumbersome to obtain information from the measurements. Further, it may not be possible to obtain exact results, analytic or numerical, for all shapes, sizes and

mismatch parameters. To overcome these hurdles, a way out is to employ approximate methods. These methods relate experimental measurements to physical properties of the scatterer in a simple and transparent way and could be the only possible alternative for the analysis of scattering pattern for particles of shapes for which exact solutions are not available.

One of the extensively used approximations to describe the scattering measurements is the Born approximation<sup>16,18</sup> (BA). The approximation is known to yield good results for weak scatterers. A simple modification to BA, termed as modified BA (MBA), was recently proposed by us<sup>18,19</sup>. This modified form is based on an analogous version of the BA in the context of scattering of light by a dielectric sphere<sup>20</sup> and an infinitely long cylinder<sup>21</sup>. Theoretically, the validity conditions for BA and MBA coincide. Therefore, their validity domains were contrasted numerically<sup>18,19</sup>. Scattering of plane and pulsed plane waves by a homogeneous sphere were considered. Detailed comparisons were made for forward and backscattering in case of plane waves and for pulse intensity integral and for maximum value of positive

\*This work was done at Saha Institute of Nuclear Physics, 1/AF, Bidhan Nagar, Kolkata 700 064

peak pressure of scattered pulse in case of pulsed plane wave. Angular scattering pattern was also compared for some particle sizes in case of plane wave scattering. As expected, MBA showed larger validity domain in comparison to BA.

A number of techniques have been employed to obtain size information using ultrasound scattering within the framework<sup>3,10,11,22</sup> of the BA. In the present paper, our aim is to examine the role of MBA in size determination of a single isolated scatterer. We examine this for two techniques. (i) It is well known in light scattering problems that angular positions of minima in a scattering pattern can be related to the scattering parameters and thus to size of the scatterer<sup>23</sup>. In this paper, we use one such technique for ultrasound scattering. The relevant relationships in the framework of BA are independent of relative density and compressibility of the scatterer and the surrounding medium. On the other hand, corresponding expression in MBA are dependent on relative density and compressibility and hence, are expected to yield more accurate results and wider validity domain. (ii) One can also extract the scatterer size information from the positions of minima of the power spectrum associated with a scattered pulse at any direction when the incident wave is a pulsed plane wave. In this method, size is estimated by analyzing the back scattered power spectrum (BSPS). We examine, numerically, the accuracy of MBA in size determination and compare with errors involved in BA for both the techniques.

## 2 Plane Wave Scattering

### 2.1 Scattering by a sphere

The scattering amplitude for the scattering of a plane acoustic wave by a sphere in partial wave analysis can be written<sup>16</sup> as:

$$\Phi_{ex}(k, \theta) = \frac{i}{k} \sum_m (2m+1) b_m P_m(\cos \theta) \quad \dots(1)$$

where

$$b_m = \frac{j'_m(x)j_m(y) - \alpha j_m(x)j'_m(y)}{h'_m(x)j_m(y) - \alpha h_m(x)j'_m(y)} \quad \dots(2)$$

Here,  $j_m$  and  $h_m$  are the spherical Bessel and Hankel function of order  $m$  and primes denote derivative with respect to their arguments, respectively. The

arguments are  $x = ka$  and  $y = nka = k_s a$  where  $k$  and  $k_s$  are the wave numbers inside and outside of the scatterer, respectively ( $a$  being the radius of the scatterer). Here,  $n$  is given by,  $n = k_s/k$ . The impedance mismatch parameter  $\alpha$  is given by  $\alpha = \eta(\rho/\rho_e)$  where  $\rho$  and  $\rho_e$  are the density of the ambient medium and of the scattering region, respectively. The direction of the observer ( $k_s$ ) makes an angle  $\theta$  with respect to the incident wave ( $k$ ). Finally,  $P_m$  is the Legendre polynomial of order  $m$ . Subscript  $ex$  in Eq. (1) refers to the exact solution.

The scattering amplitude in the Born approximation is written as<sup>16</sup>:

$$\Phi_b(k, \theta) = \frac{x^2}{q} [\gamma_k + \gamma_\rho \cos \theta] j_1(qa), \quad \dots(3)$$

where,  $\gamma_k = (k_s - k)/k$  and  $\gamma_\rho = (\rho_e - \rho)/\rho_e$  are the parameters defining mismatch of compressibility and density, respectively with  $j_1$  as the spherical Bessel function of first order. Further,  $q = k - k_s$  is the transfer of wave vector with its magnitude given by  $q = 2ks \sin(\theta/2)$  and the subscript  $b$  refers to the Born approximation. In the derivation of Eq. (3), it is assumed that the unknown field within the scatterer is the same as the incident field [ $\exp(ik \cdot r)$ ]. Thus, this result is valid for the case of weak scatterer. Theoretically, the conditions for the validity of BA are:

$$|\gamma_k| \ll 1 \quad |\gamma_\rho| \ll 1, \quad \dots(4a)$$

$$x|\gamma_k| \ll 1 \quad x|\gamma_\rho| \ll 1. \quad \dots(4b)$$

It is clear from Eq. (4b) that for a weak scatterer, the approximation can be valid even for particles that are larger than the wavelength of the incident wave. We refer to this size range as intermediate size range. For smaller particles, one can use the Rayleigh or the long wavelength approximation<sup>16</sup>.

In MBA, the scattering amplitude takes the form<sup>18</sup>:

$$\Phi_{mb}(k, \theta) = \frac{x^2}{R} [\gamma_k + n\gamma_\rho \cos \theta] j_1(Ra) \quad \dots(5)$$

Where  $R = K_s - nk$  and its magnitude is  $R = k \sqrt{1+n^2 - 2n \cos \theta}$ . The subscript  $mb$  indicates the modified Born approximation. Here,  $n$  appears in

the formula because the unknown pressure field within the scattering region is assumed to be  $\exp(ink.r)$  instead of  $\exp(ik.r)$  as in BA. This choice makes the field inside the scattering region dependent on the material properties of the scatterer. The validity domain of this approximation remains the same and is also given by Eq. (4).

It may be noted that the scattering amplitude in Eq. (3) or in Eq. (5) contains  $j_1$ . Thus, there are certain angles in the scattering pattern where the scattered intensity  $|\Phi(k, \theta)|^2$  becomes zero. These angles correspond to minima in the scattering pattern. The first three minima are given by the relations  $x_1 \approx 4.49$ ,  $x_2 \approx 7.72$ ,  $x_3 \approx 10.90$ , where,  $x_1$ ,  $x_2$ ,  $x_3$  are the corresponding arguments of  $j_1$ . Therefore, one can easily find the size of the scatterer if the angle  $\theta$  of a particular minimum is known. From the first minimum, we can write the estimated size through BA as:

$$a_{b1} = \frac{4.49}{2k \sin(\frac{\theta_1}{2})}, \quad \dots(6)$$

Subscript  $b1$  corresponds to the estimated radius employing BA in conjunction with first minimum. Similarly, using Eq. (5) for MBA, size of the scatterer can be obtained from the following relation

$$a_{mb1} = \frac{4.49}{k(1+n^2 - 2n \cos \theta_1)^{1/2}}, \quad \dots(7)$$

Eq. (7) is useful for size determination if one knows the value of  $n$  and the scattering angle  $\theta_1$ . Note that Eq. (7) is identical to Eq. (6) for  $n=1$ . That is, as  $n \rightarrow 1$ , the results from MBA and BA approach each other.

The scatterer size may be estimated from higher order minima too. For second minimum, we have:

$$a_{mb2} = \frac{7.72}{k(1+n^2 - 2n \cos \theta_2)^{1/2}}, \quad \dots(8)$$

Eqs (7) and (8) suggest that  $n$  and  $x$  can be determined simultaneously from the knowledge of any two minima positions in the scattering pattern. However, when this possibility was examined, it was found that at times this yielded a complex value of  $n$ , even for a real  $n$  scattering pattern. It was concluded

that MBA is not accurate enough for determination of  $n$ . But, as we shall see later, its estimation of  $x$  is quite accurate.

The scattered intensity can also become zero if the condition:

$$\gamma_k + \gamma_p \cos \theta = 0, \quad \dots(9)$$

for BA and the condition

$$\gamma_k + n\gamma_s \cos \theta = 0, \quad \dots(10)$$

for MBA are satisfied. That is, there is an angle where scattered intensity has a minimum that is dependent only on the material properties of the scatterer and not on its size. We call this angle the material minimum. A potential application of this minimum is that it may be used to find either density or compressibility of the scatterer if one or other is known.

## 2.2 Scattering by a long cylinder

Scattering by an infinitely long homogeneous cylinder is essentially a two-dimensional problem and for the perpendicular incidence of the input beam the scattering amplitude in terms of trigonometric series is given<sup>16</sup> by:

$$f_{sx}(\varphi) = \sqrt{\frac{2}{\pi k i}} \sum_m \varepsilon_m b_m \cos m\varphi, \quad \dots(11)$$

where  $\varepsilon_m = 1$  for  $m=0$  else  $\varepsilon_m = 2$  and

$$b_m = - \frac{J_m(x)J_m(y) - \alpha J'_m(y)J_m(x)}{H'_m(x)J_m(y) - \alpha J'_m(y)H_m(x)}, \quad \dots(12)$$

Here,  $J_m$  and  $H_m$  are respectively the Bessel and Hankel function of  $m^{\text{th}}$  order. The primes over the functions denote the derivatives with respect to their arguments.

In the Born approximation, the angle distribution factor can be written<sup>16</sup> as:

$$f_b(\varphi) = \frac{i\pi}{2} \sqrt{\frac{2}{\pi k i}} k^2 a [\gamma_k + \gamma_p \cos \varphi] \frac{J_1(qa)}{q}, \quad \dots(13)$$

where  $\vec{q} = \vec{k}_s - \vec{k}$  with its magnitude  $q = 2k \sin(\theta/2)$ . By proceeding in a similar manner as in Eq. (13), one can obtain the scattering amplitude in MBA as:

$$f_{mb}(\varphi) = \frac{i\pi}{2} \sqrt{\frac{2}{\pi k_i}} k^2 a [\gamma_k + n\gamma_\varphi \cos \varphi] \frac{J_1(Ra)}{R} \quad \dots(14)$$

where  $\vec{R} = \vec{k}_s - n\vec{k}$  with its magnitude  $R = k\sqrt{1+n^2 - 2n\cos(\theta)}$

First three zeros of  $J_1$  occur at argument values  $x_1 = 3.83$  or  $x_2 = 7.01$  or  $x_3 = 10.71$ . As a result, the formulas for size determination in BA and MBA in conjunction with first minimum may be written as:

$$a_{b1} = \frac{3.83}{2k \sin(\frac{\varphi_1}{2})}, \quad \dots(15)$$

and

$$a_{mb1} = \frac{3.83}{k(1+n^2 - 2n\cos\varphi_1)^{1/2}}, \quad \dots(16)$$

respectively. From Eq. (15), scatterer size can be estimated from the knowledge of the position of the first minimum. For size determination from Eq. (16), additional information  $n$  is required.

### 3 Pulsed Plane Wave Scattering

A pulse propagated by a real transducer can be approximated as a Gaussian wave packet<sup>24</sup> i.e., the envelop of the pulse is Gaussian. Though in the time domain, tailing edge of the pulse falls slowly compared to its leading edge so as to maintain the causality condition. In this paper, we assume that the input pulse is a Gaussian wave packet and its spatial frequency domain amplitude distribution is represented by:

$$\tilde{p}^{(in)}(k) = \left(\frac{1}{\pi\sigma^2}\right)^{1/4} \sigma \exp\left[-\frac{(k-k_0)^2\sigma^2}{2}\right] \exp[ik\mu] \quad \dots(17)$$

where  $k_0$  is the centre frequency of the wave packet with its standard deviation ( $1/\sigma$ ). The coefficient is chosen in such a way that the total energy of the input signal is equal to unity. The phase term  $\exp(ik\mu)$  tells us that the pulse at time  $t = 0$  is located at  $z = -\mu$  if  $z$  is the axis of propagation of the pulse.

Superscript  $(in)$  is used to denote the input pulse. The incident pressure pulse is given by:

$$p^{(in)}(z, t) = \frac{1}{\sqrt{2\pi}} \int_{-\infty}^{\infty} \tilde{p}^{(in)}(k) e^{ik(z-ct)} dk. \quad \dots(18)$$

The Pulse Intensity Integral (PII), defined as the time integral of the instantaneous intensity<sup>25</sup>, for the input pressure pulse at a given point  $z$  is:

$$PII^{(in)}(z) = \frac{1}{2} \int_{-\infty}^{\infty} p^{(in)}(z, t) \frac{p^{(in)*}(z, t)}{\rho c} dt, \quad \dots(19)$$

where  $*$  denotes complex conjugate of the function and  $c$  is the sound speed in the ambient medium. Though the limits of the integration are from  $-\infty$  to  $\infty$ , in the real experimental situation, in general, they can be truncated to finite limits<sup>25</sup> without losing any significant information. Moreover, in practice any signal is usually corrupted by the presence of electronic noise. Nevertheless, its contribution to PII can be removed to a great some extent by averaging signals over a number of frames<sup>26</sup> where each frame contain signal (noise plus desired signal) taken at a time. Integration in Eq. (19) can be carried out by using Eq. (18) to yield

$$PII^{(in)}(z) = \frac{1}{2\rho c} \int_{-\infty}^{\infty} |\tilde{p}^{(in)}(k)|^2 dk = \frac{1}{2\rho c}, \quad \dots(20)$$

which only depends upon the properties of the ambient medium for this particular choice of the input spectrum.

#### 3.1 Scattering by a sphere

The scattered pressure pulse in the asymptotic region ( $r \rightarrow \infty$ ) can be expressed as

$$p_{sx}^{(s)}(\vec{r}, t) = \int_{-\infty}^{\infty} \tilde{p}^{(in)}(k) \Phi_{sx}(k, \theta) \frac{e^{i(k|r-ct|)}}{r} dk. \quad \dots(21)$$

Superscript  $(s)$  represents the scattered wave. Once again the pulse intensity integral in the backscattered direction for the scattered pulse is given by:

$$PII_{sx}^{(s)}(\vec{r}) = \frac{PII^{(in)}}{r^2} \int_{-\infty}^{\infty} |\tilde{p}^{(in)}(k) \Phi_{sx}(k, \theta)|^2 dk. \quad \dots(22)$$

Therefore, the integrand in Eq. (22) gives the scattered intensity in the backscattered direction for a

plane wave of wave number  $k$ . The variation of  $|\tilde{p}^{(in)}(k)\Phi_{ex}(k, \pi)|^2$  with  $k$  is analogous to the power spectrum of the backscattered pressure pulse in an actual experimental situation. Similar expressions can be derived for approximate methods.

If one knows the  $k$  values for which  $|\tilde{p}^{(in)}(k)\Phi_{ex}(k, \pi)|^2$  becomes zero or minimum then the size of the scatterer can be found by using BA or MBA. From the exact results minima positions are known for various  $k$  values and therefore, average value of minima separations  $\bar{\Delta k}$  can be calculated. Thus, from BA:

$$a_{ss} = \frac{\bar{\Delta k}}{2\pi}, \quad \dots(23)$$

and from MBA

$$a_{ss} = \frac{\bar{\Delta k}}{(1+n)\pi}, \quad \dots(24)$$

where

$$\bar{\Delta k} = \frac{1}{(n_2 - n_1)} [x_{n_2} - x_{n_1}], \quad \dots(25)$$

is the mean separation between two successive minima related to the zeroes of  $j_1$ , where  $n_1$  and  $n_2$  are the outermost minima of the power spectrum, respectively. Corresponding arguments of  $j_1$  are  $x_{n_1}$  and  $x_{n_2}$ , respectively.

### 3.2 Scattering by a long cylinder

The scattered pressure pulse in the asymptotic region ( $r \rightarrow \infty$ ) can be expressed as:

$$p_{ex}^{(s)}(\vec{r}, \tau) = \int_{-\infty}^{\infty} \tilde{p}^{(in)}(k) f_{ex}(k, \omega) \frac{e^{ik(r-\tau)}}{\sqrt{r}} dk. \quad \dots(26)$$

Once again the pulse intensity integral in the backscattered direction for the scattered pulse can be derived as:

$$PII_{ex}^{(s)}(\vec{r}) = \frac{PII^{(in)}}{r} \int_{-\infty}^{\infty} |\tilde{p}^{(in)}(k)f_{ex}(k, \pi)|^2 dk \quad \dots(27)$$

The variation of  $|\tilde{p}^{(in)}(k)f_{ex}(k, \pi)|^2$  with  $k$  may be contrasted with the power spectrum of the backscattered pressure pulse in practice. Similar expressions can be derived for the approximate methods too.

If one knows the  $k$  values for which  $|\tilde{p}^{(in)}(k)f_{ex}(k, \pi)|^2$  becomes zero or minimum then the size of the scatterer can be found by using BA or MBA model as it was in Eq. (23) or Eq. (24) but the zeros are those of  $J_1$  for this case.

### 4 Numerical Comparison

The accuracy of MBA in size determination using angular scattering pattern as well as backscattering methods and compare the results so obtained with those obtained using BA are accessed. For angular scattering method we consider an incident plane wave while for the protocol employing backscattering we employ pulsed plane waves. In both methods two types of scatterer have been considered. These are homogeneous spheres and infinitely long cylinders. For both types of scatterers exact analytical solutions exist. The acoustical properties (density and compressibility) of the scattering region have been varied up to  $\pm 15\%$  with respect to the ambient medium. For our calculations we took 5 MHz as the frequency of incident plane wave. The size estimations of isolated scatterers by using approximate methods have been carried out over a large range of scatterers whose size parameters vary from 3 to 75.

The lower limit of  $x$  is chosen on the basis that at least one minimum should occur within the entire angular domain, otherwise the proposed method cannot be useful. On the other hand the upper limit has been fixed to 75 because after that the region of validity (accuracy  $< 10\%$ ) of approximations become very small. To estimate the size of the scatterer from the backscattered power spectrum we consider the scattering of two pulses each of centre frequency 5 MHz. The bandwidth (-6 dB) of the pulses are 1.406 MHz (28.12%) and 4.016 MHz (80.32%) respectively. And accordingly, two pulses are narrow band (NB) and wide band (WB) respectively with pulse durations  $\approx 562.5$  ns and  $\approx 237.5$  ns respectively.

Figure 1 shows a typical angular distribution of scattered intensity calculated using exact solution for a sphere of  $x = 22$  with  $\rho_e / \rho = 0.90$  and  $\kappa_e / \kappa = 1.10$ . As expected, scattered intensity pattern shows minima and maxima at certain angles.

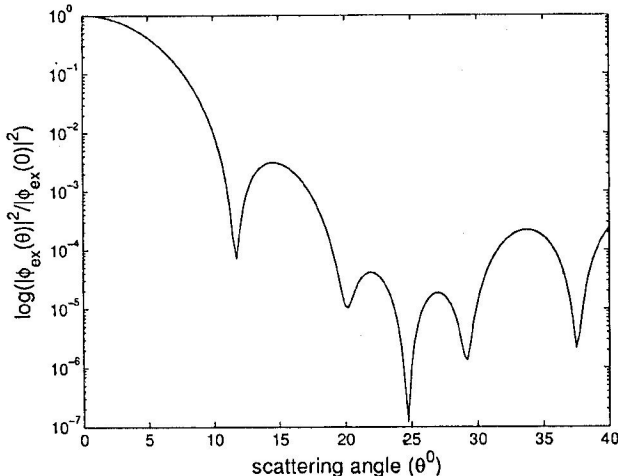


Fig. 1—Angular scattered intensity distribution for a sphere of size  $x = 22$  with  $\rho_e / \rho = 0.90$  and  $\kappa_e / \kappa = 1.10$

First few minima in this case occur at  $11.75^\circ$ ,  $20.25^\circ$ ,  $24.75^\circ$ ,  $29.25^\circ$  and  $37.50^\circ$ . From the position of these minima, size of the target can be determined. For the first minima the relations in BA and MBA are given by Eqs (6) and (7) respectively. It can be easily ascertained that the third minimum in Fig. 1 is a material minimum and thus, need not be taken into account for size calculations.

Representative error charts for BA and MBA in size determination are shown in Figures 2(a) and 2(b), respectively for a spherical scatterer with  $x = 22$ . Figure 2(c) and (d) show the corresponding bar diagrams. The error in size determination has been defined as:

$$\text{size error} = \frac{|a - a_{es}|}{a} \times 100\%, \quad \dots(28)$$

where  $a$  and  $a_{es}$  are the true size and estimated size respectively. The exact scattering pattern is obtained for a particle of given size  $a$  and than  $a_{es}$  is obtained from this scattering pattern using approximate formulas. Four different gray values have been

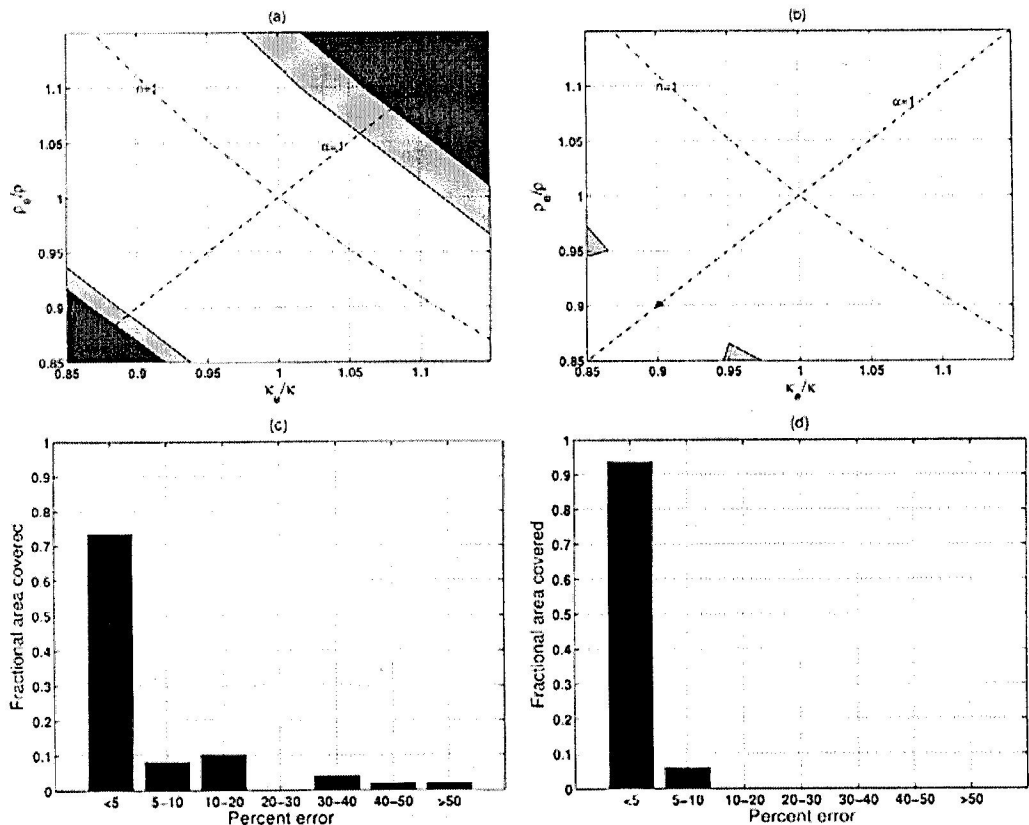


Fig. 2—(a) Error contour charts for size estimation through angular scanning in BA for  $x = 22$ . White region: error  $<5\%$ , gray region: error  $5-10\%$ , dark region: error  $10-50\%$  and darkest region: error  $>50\%$ . (b) Same as (a) but for MBA with white region: error  $<5\%$ , gray region: error  $>5\%$ . (c) Bar diagram for (a). (d) Bar diagram for (b)

attributed to mark the errors of various regions (Fig. 2). For a desired accuracy in size calculation MBA has a larger domain of validity in comparison to BA (Fig. 2). For example, if 10% is the acceptable error, MBA can be used for entire range of  $\gamma_\kappa$  and  $\gamma_\rho$  values considered here. BA on the other hand is valid with that accuracy over about 82% of the region. An important observation that can be made from Fig. 2 is that the approximations in size determination are good near  $n = 1$ . The same is not true for  $\alpha$ . The errors can be quite large even when the impedance mismatch parameter is close to 1. This implies that these approximations should be looked upon as  $n \rightarrow 1$  approximations and not as  $\alpha \rightarrow 1$  approximation.

Table 1 presents the fractional areas, normalized with respect to the whole region, with errors <5% and <10% in size determination from the first and second minimum for various size parameters of a spherical scatterer. Corresponding results for a long cylindrical scatterer are presented in Table 2. It is clear from results obtained by employing the first minimum that MBA has a larger validity domain in comparison to BA for almost all  $x$  values. The maximum  $x$  value for which an approximation can also be used also becomes larger in MBA. For example, if the error limitation is 10% then BA is valid in 80% of the region of  $(\gamma_\kappa, \gamma_\rho)$  domain if  $x \leq 22$ . But for MBA this value of  $x$  goes up to about  $x \leq 40$ . It may be noted that this value of  $x$  increases further if the size

Table 1—Size error from angular scattering pattern for spherical scatterer

Size ( $ka$ )	Fractional area covered by the error							
	From 1 <sup>st</sup> minimum				From 2 <sup>nd</sup> minimum			
	Error BA	< 5% MBA	Error BA	< 10% MBA	Error BA	< 5% MBA	Error BA	< 10% MBA
3	0.65	0.84	0.84	0.86				
5	0.80	0.92	0.96	0.96	0.57	0.82	0.84	0.90
7	0.78	0.96	0.96	0.96	0.65	0.80	0.88	0.86
10	0.76	0.94	0.92	0.98	0.76	0.92	0.92	0.92
12	0.80	0.94	0.90	0.96	0.71	0.90	0.92	0.92
15	0.69	0.88	0.88	0.94	0.73	0.90	0.90	0.92
18	0.78	0.90	0.84	0.98	0.73	0.88	0.90	0.92
20	0.80	0.84	0.86	1.00	0.76	0.88	0.88	0.90
22	0.73	0.94	0.82	1.00	0.67	0.88	0.82	0.88
25	0.57	0.92	0.67	1.00	0.63	0.88	0.82	0.90
35	0.35	0.88	0.63	0.88	0.71	0.88	0.82	0.88
50	0.39	0.63	0.45	0.76	0.63	0.80	0.63	0.80
75	0.35	0.33	0.35	0.51	0.37	0.59	0.63	0.59

Table 2—Size error from angular scattering pattern for cylindrical scatterer

Size ( $ka$ )	Fractional area covered by the error							
	From 1 <sup>st</sup> minimum				From 2 <sup>nd</sup> minimum			
	Error BA	< 5% MBA	Error BA	< 10% MBA	Error BA	< 5% MBA	Error BA	< 10% MBA
3	0.65	0.82	0.84	0.86				
5	0.80	0.98	0.98	1.00	0.57	0.73	0.84	0.82
7	0.82	0.98	0.98	1.00	0.67	0.86	0.90	0.92
10	0.78	0.94	0.96	0.98	0.73	0.92	0.94	0.96
12	0.67	0.92	0.92	0.98	0.71	0.94	0.94	0.96
15	0.82	0.88	0.88	1.00	0.71	0.94	0.92	0.94
18	0.73	0.94	0.86	1.00	0.76	0.94	0.92	0.94
20	0.73	1.00	0.82	1.00	0.67	0.88	0.88	0.94
22	0.57	0.92	0.67	1.00	0.67	0.94	0.88	0.94
25	0.49	0.96	0.67	0.96	0.67	0.88	0.82	0.94
35	0.39	0.80	0.61	0.88	0.67	0.88	0.82	0.88
50	0.45	0.51	0.45	0.63	0.45	0.67	0.63	0.76
75	0.29	0.31	0.29	0.49	0.43	0.55	0.61	0.61

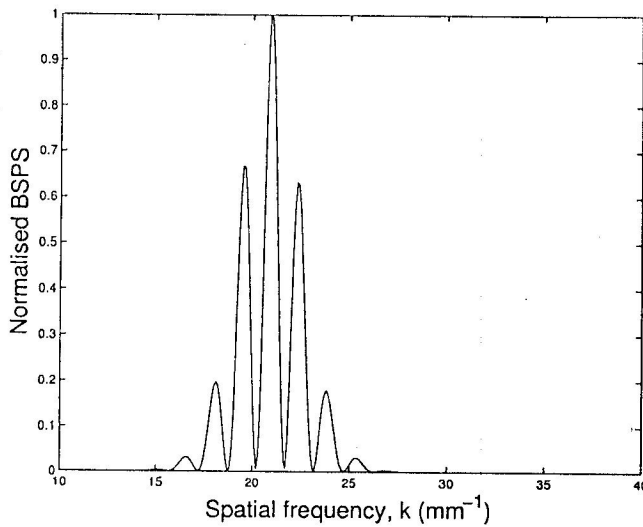


Fig. 3—Normalized backscattered power spectrum (BSPS) for a sphere of  $x = 22$  with  $\rho_e / \rho = 1.05$ ,  $\kappa_e / \kappa = 0.95\kappa$

is determined from the second minimum. In the case considered in Table 1, this value increases to about  $x = 50$  when size is obtained from the position of the second minimum. Similar trends are observed for infinitely long cylindrical particles too.

In Fig. 3, a typical plot of normalized backscattered power spectrum is displayed for  $x = 22$  with  $\rho_e / \rho = 1.05$  and  $\kappa_e / \kappa = 0.95\kappa$ . It may be seen that for some frequencies intensity becomes minimum and average value of separations of spatial frequency  $\bar{\Delta}k$  between two successive minima can be obtained from this spectra. Therefore, one can easily find out the size of a spherical target by using Eq. (23) and Eq. (24). As size decreases, lesser number of oscillations are observed in the spectrum and this in turn leads to greater error in value of  $\bar{\Delta}k$ .

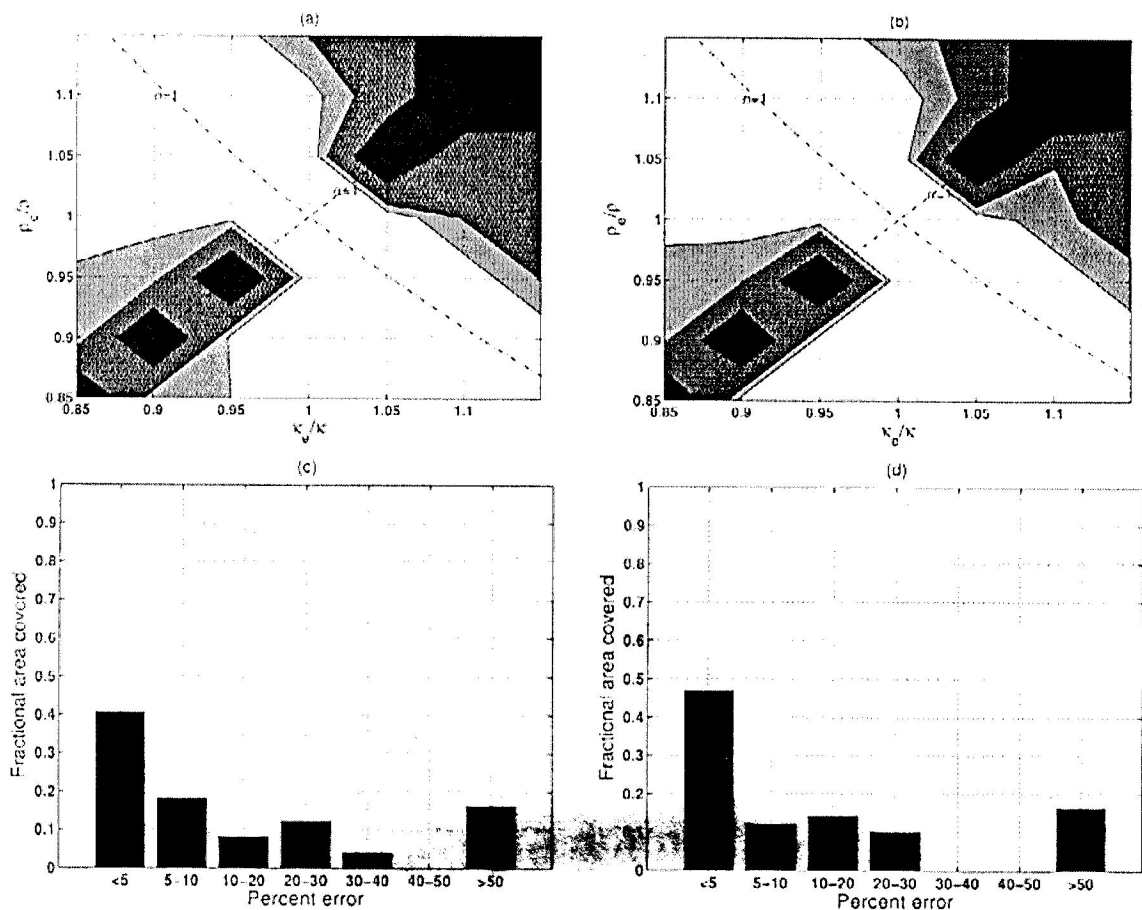


Fig. 4—(a) Error contour charts for size estimation by analyzing backscattered power spectrum (BSPS) in BA for  $x = 22$ . White region: error <10%, gray region: error 10-20%, dark region: error 20-50% and darkest region: error >50%. (b) Same as (a) but for MBA. (c) Bar diagram for (a). (d) Bar diagram for (b)

Figure 4 shows error charts in size determination in using BA and MBA when backscattered power spectrum method is used for this purpose. Corresponding bar diagrams are also included in that figure. The values of fractional areas covered by specified errors are presented in Tables 3 and 4 for various  $x$  values for spherical and infinitely long cylindrical scatterers. Results for NB pulse in Table 3 show that MBA has a larger domain of validity than BA almost in the whole particle size range. But the difference in the two is not very significant here. It is also noted that for  $x < 7$ , BA as well as MBA are valid only over a very small domain of  $(\gamma_k, \gamma_\rho)$  region. Further, as in angular scattering method, the

approximations are best for size determination near  $n = 1$ . Similar trends are observed in the case of WB pulse too. However, for small size parameters ( $x < 7$ ), WB pulse provides results better than NB pulse.

Tables 1-4 presents that, in general, the results obtained by angular scattering minima positions have larger validity domain in comparison to the backscattering method. The difference is less significant for the case of infinite cylinders. It is much more significant for the case of homogeneous spheres.

## 5 Conclusions

In this paper, we have examined the validity domain of a modified Born approximation for particle

Table 3—Size error from backscattered power spectrum for spherical scatterer

Size ( $ka$ )	Error BA	Fractional area covered by the error				From BSPS (WB Pulse)			
		< 5% MBA	Error BA	< 10% MBA	Error BA	< 5% MBA	Error BA	< 10% MBA	
3	0.24	0.14	0.35	0.37	0.33	0.55	0.59	0.78	
5	0.14	0.18	0.22	0.29	0.47	0.65	0.69	0.80	
7	0.49	0.63	0.71	0.78	0.51	0.69	0.73	0.80	
10	0.33	0.45	0.55	0.67	0.53	0.65	0.71	0.76	
12	0.43	0.53	0.65	0.71	0.51	0.61	0.73	0.71	
15	0.57	0.61	0.65	0.69	0.53	0.59	0.67	0.76	
18	0.51	0.59	0.67	0.65	0.53	0.57	0.69	0.73	
20	0.45	0.57	0.65	0.59	0.47	0.55	0.67	0.65	
22	0.41	0.47	0.59	0.59	0.47	0.51	0.67	0.63	
25	0.45	0.51	0.57	0.55	0.49	0.53	0.65	0.63	
35	0.43	0.51	0.65	0.71	0.49	0.55	0.67	0.67	
50	0.45	0.53	0.61	0.65	0.35	0.45	0.59	0.65	
75	0.14	0.20	0.37	0.39	0.18	0.16	0.35	0.37	

Table 4—Size error from backscattered power spectrum for cylindrical scatterer

Size ( $ka$ )	Error BA	Fractional area covered by the error				From BSPS (WB Pulse)			
		< 5% MBA	Error BA	< 10% MBA	Error BA	< 5% MBA	Error BA	< 10% MBA	
3	0.06	0.04	0.18	0.06	0.41	0.63	0.67	0.84	
5	0.06	0.06	0.06	0.10	0.49	0.80	0.80	0.90	
7	0.51	0.61	0.69	0.84	0.49	0.78	0.84	0.88	
10	0.51	0.71	0.71	0.80	0.49	0.73	0.80	0.86	
12	0.49	0.71	0.71	0.82	0.49	0.71	0.78	0.84	
15	0.51	0.80	0.80	0.84	0.53	0.71	0.76	0.80	
18	0.49	0.76	0.78	0.84	0.57	0.71	0.76	0.84	
20	0.49	0.76	0.76	0.80	0.49	0.67	0.73	0.80	
22	0.45	0.69	0.69	0.78	0.51	0.71	0.76	0.80	
25	0.55	0.73	0.78	0.82	0.49	0.71	0.73	0.84	
35	0.45	0.69	0.71	0.82	0.49	0.67	0.69	0.80	
50	0.45	0.63	0.67	0.73	0.47	0.63	0.63	0.74	
75	0.14	0.16	0.20	0.20	0.12	0.16	0.29	0.24	

sizing and compared the results so obtained with those obtained by using the conventional Born approximation. The target considered here is an isolated scatterer whose size is larger than the wavelength of the interrogating waves (Mie scatterers). Two methods have been used and compared. One is based on the analysis of angular scattering data and the other is based on the analysis of backscattered power spectrum. Two test cases have been considered. These are scattering by a homogeneous sphere and scattering by an infinitely long cylinder. Exact solutions are available for these test cases. Following conclusions emerge from the present investigation:

- (i) If the scattering is weak and provided the particle size parameter is not very large, BA as well as MBA lead to reasonably good assessment of the size of the scatterer. Comparatively, results from MBA are superior. The upper size limit for the validity of these approximations depends on  $\alpha$  and  $n$  and the accuracy desired. The limit also depends on which minimum is being used for the extraction of information. General trend seems to be - higher the order of minima, higher is the upper limit.
- (ii) It is noted that the approximations should be looked upon as  $n \rightarrow 1$  approximations and not as small impedance mismatch ( $\alpha \rightarrow 1$ ) approximations. That is, the mismatch in density and compressibility should be small individually.
- (iii) MBA has significantly larger domain of validity in comparison to BA [that is, for the same maximum per cent error, MBA is generally valid for larger values of  $(\gamma_\kappa, \gamma_\rho)$  parameters as well as larger sizes]. For example, in angular scattering method for a sphere, the MBA has less than 5% error in more than 80% of  $(\gamma_\kappa, \gamma_\rho)$  domain for  $x \leq 35$ . The corresponding domain for the BA is only 35% of total  $(\gamma_\kappa, \gamma_\rho)$  domain.
- (iv) Angular scattering method has larger validity domain in comparison to the backscattered power spectrum method. Thus, the angular scattering method is preferable whenever situation allows it to be employed. The

difference in the two methods is noted to be larger for spheres than that for infinitely long cylinders.

- (v) If angular scattering data is to be employed for size determination the first minimum should be within  $180^\circ$ . For BA this means that minimum size of a spherical scatterer that can be determined is  $x \approx 2.245$ . Similarly for an infinite cylinder this limit is  $x \approx 1.915$ . On the other hand, these lower limits of sizes vary in MBA depending upon the material properties of the particles.

## References

1. Lizzi F L, Greenebaum M, Feleppa E J, Elbaum M & Coleman D J, *J Acoust Soc Am*, 73 (1983) 1366.
2. Insana M F, Wagner R F, Brown D G & Hall T J, *J Acoust Soc Am*, 87 (1990) 179.
3. Shung K K & Theine G A, *Ultrasonic scattering in biological tissues*, (CRC Press) 1993.
4. Epstein P S & Charat R R, *J Acoust Soc Am*, 25 (1953) 553.
5. Allegra J R & Hawley S A, *J Acoust Soc Am*, 51 (1972) 1545.
6. Dukhin A S & Goetz P J, *Ultrasound for Characterizing Colloids*, (Elsevier Academic Press) 2002.
7. Stanton T K, Chu D & Wiebe P H, *J Acoust Soc Am*, 103 (1998) 236.
8. Kitamura K, Pan H, Ueha S, Kimura S & Ohtomo N, *Jpn J Appl Phys*, 35 (1996) 3156.
9. Kitamura K, Nishikouri H, Ueha S, Kimura S & Ohtomo N, *Jpn J Appl Phys*, 37 (1998) 3082.
10. Lacefield J C & von Ramm O T, *J Acoust Soc Am*, 108 (2000) 1914.
11. Mast T D & Waag R C, *J Acoust Soc Am*, 98 (1998) 3050.
12. Flax L, Dragnoette L R & Uberrall H, *J Acoust Soc Am*, 63 (1978) 723.
13. Brill D & Gaunard G C, *J Acoust Soc Am*, 73 (1983) 1448.
14. Mathieu J, Schweitzer P & Tisser E, *Measurement Science & Technology*, 13 (2002) 660.
15. Chu D & Ye Z, *J Acoust Soc Am*, 106 (1999) 1732.
16. Morse P M & Ingard K U, *Theoretical Acoustics*, (McGraw-Hill: New York), 1968.
17. Faran J J, *J Acoust Soc Am*, 23 (1951) 405.
18. Sharma S K & Saha R K, *Waves in random media*, 14 (2004) 525.
19. Saha R K & Sharma S K, *Phy Med Bio*, 50 (2005) 2823.
20. Shimizu K, *J Opt Soc Am*, 73 (1983) 504.
21. Sharma S K & Somerford D J, *J Phys D: Appl Phys*, 21 (1988) 139.
22. Coussios C, *J Acoust Soc Am*, 112 (2002) 906.
23. Sharma S K & Somerford D J, *Light scattering by optically soft scatterers: Theory & applications*, (Springer-Praxis: UK) 2006.
24. Szabo T L, *Diagnostic Ultrasound Imaging: Inside Out*, (Elsevier Academic Press) 2004.
25. Raum K & O'Brien W D, *IEEE TransUFFC*, 44 (1997) 810.
26. Li Y, Chen Q & Zagzebski J A, *IEEE Trans UFFC*, 51 (2004).